HHS Public Access

Author manuscript

J Control Release. Author manuscript; available in PMC 2021 May 10.

Published in final edited form as:

J Control Release. 2020 May 10; 321: 272–284. doi:10.1016/j.jconrel.2020.01.051.

Ultrasound-Mediated Delivery of miRNA-122 and Anti-miRNA-21 Therapeutically Immunomodulates Murine Hepatocellular Carcinoma *In Vivo*

Jennifer C. Wischhusen[1,2], **Sayan Mullick Chowdhury**[2], **Taehwa Lee**[2], **Huaijun Wang**[2], **Sunitha Bachawal**[2], **Rammohan Devulapally**[2], **Rayhaneh Afjei**[2], **Uday Kumar Sukumar**[2], **Ramasamy Paulmurugan**[2,*]

[1]Apoptosis, Cancer and Development Laboratory, Centre de Cancérologie de Lyon, INSERM U1052-CNRS UMR5286, Centre Léon Bérard, 69008 Lyon, France

[2]Department of Radiology, School of Medicine, Stanford University, Stanford, CA, USA

Abstract

Hepatocellular carcinoma (HCC) is the most common cause of cancer-related mortality, and patients with HCC show poor response to currently available treatments, which demands new therapies. We recently developed a synthetic microRNA-based molecularly targeted therapy for improving HCC response to chemotherapy by eliminating drug resistance. We used ultrasound-targeted microbubble destruction (UTMD) to locally deliver microRNA-loaded nanoparticles to HCC. Since the immune microenvironment plays a crucial role in HCC disease development and response to treatment, and UTMD and microRNAs have the potential to interfere with the immune system, in this study we analyzed the immunomodulatory effects of UTMD and miRNAs in HCC. We used an immunocompetent syngeneic HCC mouse model for the study. We conducted cytokine profiling in tumor, lymph nodes, and serum of animals within the first 24 h of treatment to analyze changes in the level of pro- and antitumoral cytokines. The results showed: (1) Hepa1–6 syngeneic tumors expressed HCC-related cytokines, (2) UTMD-microRNA combination therapy triggered transient cytokine storms, and (3) delivery of microRNA-122 and anti-microRNA-21 affected the immune microenvironment by decreasing the level of GM-CSF in tumors while modulating protumoral IL-1α, IL-1β, IL-5, IL-6 and IL-17 and antitumoral IL-2 and IL-12 in tumor-proximal lymph nodes, and increasing IL-2 in the serum of tumor-bearing mice. Local delivery of targeted

[*]**Contact information** Ramasamy Paulmurugan, Canary Center @ Stanford for Cancer Early Detection, 3155 Porter Dr, Palo Alto, CA 94304, USA, Tel: +1 650 725-6097, Fax: +1 650 721-6921, paulmur8@stanford.edu.

Author contributions (using relevant CRediT roles)

1. Jennifer Wischhusen: Conceptualization, data curation, formal analysis, methodology, writing the original draft
2. Sayan Mullick Chowdhury: Data curation
3. Taehwa Lee: Data curation
4. Huaijun Wang: Formal analysis
5. Sunitha Bachawal: Methodology
6. Rammohan Devulapally: Methodology
7. Rayhaneh Afjei: Data curation
8. Uday Kumar Sukumar: Data curation
9. Ramasamy Paulmurugan: Conceptualization, funding acquisition, project administration, supervision, review & editing

therapy by UTMD significantly reduced the concentration of IL-12 and IL-17 in lymph nodes of treated and contralateral tumors suggesting a systemic response.

Conclusion—UTMD-mediated delivery of microRNA-122 and anti-microRNA-21 modulated the immune microenvironment of Hepa1–6 tumors at the level of cytokine expressions. Exploiting antitumoral immune effects could enhance the therapeutic efficacy of the proposed combination therapy for HCC.

Keywords

Ultrasound-targeted microbubble destruction; local drug delivery; poly (lactic-*co*-glycolic acid) nanoparticles; cytokine screening; tumor immune response

Introduction

Hepatocellular carcinoma (HCC) is the seventh most common cancer worldwide and the second leading cause of cancer-related death (1). The current treatment paradigm for HCC has significant limitations. While early stage HCC is treatable by surgical resection or liver transplantation, with local thermal ablation as an alternative (2,3), only 10–30% of patients qualify for surgical management (4); recurrence is common after resection (up to 70%) (5), and transplantation is limited by a shortage of donor organs. For intermediate stage HCC, transarterial chemoembolization (TACE) is the standard of care (6), with transarterial radioembolization is emerging as a complementary liver-directed therapy (7). Unfortunately, both are often contraindicated in cirrhotic patients due to poor baseline liver function and treatment response can be variable. Patients with advanced HCC and those who fail or are ineligible for liver-directed therapies are left with extremely limited treatment options and dismal prognosis. Moreover, HCC is commonly resistant to chemotherapies, such as doxorubicin (8). Despite screening, most HCC patients are diagnosed at intermediate or advanced stage with large/multifocal lesions, extrahepatic spread, and vascular invasion (1). These patients are excluded from surgery and undergo palliative therapy such as local chemotherapy (transarterial chemoembolization), or with sorafenib, a small molecule kinase inhibitor, for which the response rates are low and side effects are common (1,9). Thus, novel therapies for intermediate and advanced stage patients are required to improve disease management.

Targeted delivery using various nanoparticles have been used for small molecule drugs and siRNAs. Doxorubicin with liposome as a nanocomplex (Doxil) is currently used for cancer therapy in the clinic to reduce non-specific toxicity associated with Doxorubicin. In contrast to all the advances in various delivery approaches and therapeutic molecules, immunotherapy has been dominating as a promising treatment for various cancers. But not many immunotherapies are currently available for HCC, except the recently tested PD-1 inhibitory monoclonal antibodies, such as pembrolizumab and nivolumab, as a second-line therapy for advanced HCC as monotherapy (10). Hence, our group has previously reported a novel therapeutic approach for HCC using an image-guided focused ultrasound (US)-based system for localized delivery of miRNA-loaded poly (lactic-*co*-glycolic acid) nanoparticles (PLGA-NPs) and subsequent systemic chemotherapy with doxorubicin (Dox) to reduce the dose of Dox needed for treatment (11,12). US drug delivery was achieved by intravenous

injection of contrast agents called microbubbles (MBs), with a diameter of 1–5 μm, and the application of US to trigger targeted MB destruction (UTMD) causing MB oscillation and collapse (13). This process, termed cavitation, permeabilizes treated tissue thereby facilitating the delivery of co-injected drugs/drug loaded nanoparticles, such as PLGA-NPs, to the tumor. Our PLGA-NPs are loaded with microRNA-122 (miR-122) and anti-microRNA-21 (anti-miR-21). miR-122 is a tumor suppressor microRNA (miRNA) that is downregulated in HCC causing apoptosis evasion, tumor progression, metastasis and drug resistance (14,15). In contrast, miR-21 is an oncogenic miRNA that is upregulated in HCC and promotes tumor cell proliferation, migration, invasion and chemo-resistance (16,17). The combination treatment with miR-122 and anti-miR-21 complements the lack of miR-122 while decreasing the level of endogenous miR-21 by functional inhibition in HepG2 human HCC cells, and this process molecularly alter the endogenous target genes expression to implement therapeutic response (12). Therefore, this approach is considered a molecularly targeted therapy affecting cancer cells with altered miR-122 and miR-21 expression. The complementary miRNA therapy re-sensitizes HCC to Dox and shows improved therapeutic efficacy (12). These results underscore its potential for further development.

The immune system plays an important role in HCC disease that is an antigenic lesion expressing tumor-associated antigens and neo-antigens leading to infiltration of tumor-associated antigen-specific $CD8^+$ T-cells (18). But tumor cell recognition by $CD8^+$ T-cells is prevented by regulatory T cells, myeloid-derived suppressor cells, and tumor-associated (M2) macrophages, and immune checkpoint regulators expressed by tumor cells (18,19). In order to challenge HCC, this protumoral immune barrier needs to be thwarted.

miR-122, miR-21, and UTMD have been reported to modulate the immune system. miR-122 downregulation in HCC upregulates monocyte chemoattractant protein 1 (MCP-1) supporting the pro-inflammatory environment required for HCC progression. Hence, delivery of miR-122 is expected to attenuate or revert this condition (20,21). Myeloid-derived suppressor cells and HCC cells overexpress miR-21, which limits the polarization of antitumoral Th1 cells. This in turn activates anti-inflammatory M2 macrophages and promote pro-inflammatory and protumoral microenvironment (22,23), which is expected to be inhibited by the delivery of anti-miR-21. It has been previously shown in colorectal tumor models that mechanical or low-intensity US can induce the leakage of antigens and molecules from tumor cells leading to recruitment and accumulation of cytotoxic T cells and Natural Killer cells in the tumor (24,25). Similarly, immunogenic presentation of tumor antigens and the reversal of T cell tolerance has been shown in a melanoma model (26). Thus, in this study, we sought to evaluate whether our proposed combination therapy has any immune-modulatory activity in an immune-competent syngeneic murine HCC model, which can be exploited to enhance anti-cancer therapeutic efficacy. To do so, we applied UTMD alone or UTMD in combination with miRNA and assessed the associated change in the immune microenvironment of the tumor, tumor-proximal lymph nodes, and serum by screening for an array of pro- and antitumoral cytokines (Fig. 1A). We observed a significant change in the expression level of antitumoral cytokines when we used UTMD in combination with microRNAs compared untreated conditions.

Materials and Methods

PREPARATION OF miRNA-LOADED PLGA-*b*-PEG NANOPARTICLES

miRNA-loaded PLGA-PEG NPs were prepared as described by us previously (11,12,27,28). For more details, refer to the Supplementary Material and Methods. Of note, we used the same miR-122 and anti-miR-21 sequences as used for drug delivery to human HCC since the mature miRNA sequences of both human and murine are identical (Supp. Tab. S1).

IN VITRO EXPERIMENTS

Therapeutic response of Hepa1–6 (CRL-1830, ATCC) murine HCC cells to miRNA-122/anti-miR-21 treatment was assessed by measuring cell viability by propidium iodide staining based FACS analysis, western blot analysis for the expression of pro- and anti-apoptotic proteins, and the cellular levels of miR-122 and anti-miR-21 upon treatment. The in vitro experiments are described in more detail in Supplementary Material and Methods.

ANIMAL STUDIES

The Institutional Administrative Panel on Laboratory Animal Care at Stanford University approved all procedures involving the use of laboratory animals. C57BL/6J mice were purchased from The Jackson Laboratory (Bar Harbor, ME, USA). A total of 4 million Hepa1–6 cells of an early passage (less than 5) were subcutaneously injected into the lower flank of 8-weeks old female C57BL/6J mice. After four weeks, tumors were surgically excised and pieces (~0.1 mm) of the first established Hepa1–6 tumor were further engrafted using a Precision Trochar (Innovative Research of America, Sarasota, Florida, USA) under sterile conditions. This procedure was repeated for establishing a syngeneic Hepa1–6 HCC mouse model for further experiments. Mice at the age of 12 weeks with a fully active immune system were used for all the experiments conducted in this study.

US THERAPY SYSTEM

The composite US system used for local UTMD treatment was previously described (Lee et al., under revision). Briefly, each tumor was perfused with MBs and miRNA-loaded NPs and insonified five times in total. During each therapy cycle, the US transducer was electronically steered into six adjacent foci to cover the entire tumor volume (Fig. 1B). The detailed procedure for UTMD is described in Supplementary Material and Methods.

THERAPY RESPONSE ASSESSMENT

To assess the efficacy of the combination therapy approach, Hepa1–6 tumors were treated with UTMD + miRNA followed by an intraperitoneal injection of doxorubicin at 10 mg/kg body weight on day 0, 1 and 3. Tumor volume was measured with a caliper, and the apoptosis was assessed by TUNEL assay as described in detail in Supplementary Material and Methods.

CYTOKINE EXPRESSION ANALYSIS

For cytokine expression analysis, serum, lymph nodes, muscles and tumor samples were collected at 0.5 h, 6 h, and 24 h after UTMD or UTMD/miRNA treatment (Fig. 1C). Mice

were kept under anesthesia at 2% isoflurane in oxygen (2 L/min) during treatment and blood collection. Blood was collected by submandibular bleeding into Serum Gel Z/1.1 tubes. Tubes were kept at room temperature for 15 min to allow clotting, and centrifuged for 5 min at 5,000 rpm. Supernatants were collected and stored at −80 °C until the assay was performed. To remove blood pool associated cytokines in tumors and lymph nodes, mice underwent cardiac perfusion with 15 mL of phosphate buffer saline. Then, inguinal lymph nodes of treated and contralateral sites were isolated. Finally, treated and contralateral control tumors or hind limb muscle were collected. All tissues were flash frozen in liquid nitrogen and finally stored at −80 °C until processing. To isolate proteins from tissues, 100 μL of lysis buffer was added to 50 mg of tissues, and tissues were homogenized (PRO250 Homogenizer, PRO Scientific) for approximately 1 min at intermediate speed. Samples were centrifuged at 10,000 rpm for 5 min at 4 °C and supernatants were collected for use in cytokine assays. Protein concentrations were quantified by Bio-Rad Protein Assay kit and Qubit Protein Assay Kit. 16-plex Q-Plex Array (Quansys Biosciences, Logan, Utah, USA) was used to screen a panel of pro- and antitumoral cytokines (IL-1α, IL-1β, IL-2, IL-3, IL-4, IL-5, IL-6, IL-10, IL-12, IL-17, MCP-1, IFN-γ, TNF-α, MIP-1α, GM-CSF, and RANTES) (Fig. 1C). For tissue samples, 125 μg of protein was used for the assay. For serum, the samples were diluted 1:2 prior to use. Read-out of Q-Plex 96-well plates was performed using an IVIS Lumina III (Caliper Life Sciences, Perkin Elmer, Waltham, MA) optical imaging system. Absolute photon counts were acquired, regions of interest were manually positioned over the chemiluminescent signals, and the photon counts of the calibrator and samples were used to calculate the concentration of cytokines in pg/mL that were above the limit of quantification (Supp. Tab. S2).

STATISTICAL ANALYSIS

All continuous measurements were expressed as mean ± standard error of mean (SEM). The two-sample Wilcoxon rank test was used for comparisons between two groups for data collected in the tumor growth study, TUNEL assay, and cytokine screening. All treated or intra-animal contralateral control tissues were compared to untreated control tissues as listed in detail in the Supplementary Material and Methods. All statistical analyses were performed with statistical software (SPSS version 21; IBM Corporation, Endicott, NY). Asterisks indicate significant differences with *: $p<0.05$ or **: $p<0.01$.

Results

miR-122 AND anti-miR-21 CO-TREATMENT TO HCC CELLS DECREASE CELL VIABILITY AND INCREASE APOPTOSIS *IN VITRO*

We sought to assess the immune-modulatory function of UTMD-mediated miRNA delivery to leverage it as a novel therapy approach for HCC. First, we tested the *in vitro* response of murine Hepa1–6 cells to the combined treatment with miR-122- and anti-miR-21-loaded PLGA-PEG NPs and Dox (Fig. 2A). Incubation of cells with a combination of miRNA-loaded NPs showed microRNA dose-dependent decrease in cell viability in the presence and absence of doxorubicin (Supp. Fig. S1A). Incubation of cells with miRNA-loaded NPs (10 pmols each of miR-122 and anti-miR-21) led to a decrease in the viable cell population from 89% in the control to 66.8% in miR-122/anti-miR-21-treated cells (Fig. 2B). When miRNA

treatment was combined with 1 μM Dox, cell viability further decreased from 83.9% in the Dox alone treatment to 49.8% after miRNA/Dox co-treatment. We also assessed the cell cycle status of different treatment conditions. The microRNA co-treatment in presence and absence of Dox enhanced cell cycle arrest at S/G2 phases, and sensitized cells to Dox-mediated apoptosis (Fig. 2C,D and Supp. Fig. S1B).

Next, the intracellular delivery of intact miRNAs was assessed by real time quantitative RT-PCR. The results showed successful delivery of miRNAs in Hepa1–6 cells, which was $1.5\pm0.5\times10^5$-fold (miR-122) and $3.5\pm0.7\times10^5$-fold (anti-miR-21) higher in cells treated with respective miRNAs either treated alone or in combination with Dox (Fig. 3A–C). Treatment with Dox did not affect the transfection efficiency of miRNAs (Fig. 3C). Further, the expression of pro- and antiapoptotic proteins along with the targets of miR-122 and miR-21 were assessed. PDCD4 and PTEN, both inhibited by oncomiR-21, were upregulated upon anti-miR-21 treatment confirming successful delivery and activity of anti-miR-21 in Hepa1–6 cells (Fig. 3D). The expression of survival factor IGF-1R and cell cycle inhibitor p21 did not change much upon treatment. Pro-apoptotic Puma protein was slightly decreased when co-treated with miRNA/Dox. The survival factor Bcl2 but also the pro-apoptotic protein BAX were decreased in cells treated with miR-122/anti-miR-21/Dox compared with the control condition but the BAX to Bcl2 ratio increased which supported the apoptotic action in cells.

Taken together, there was an overall positive *in vitro* therapy response decreasing cell viability, confirming successful miRNA delivery and increasing pro-apoptotic activities.

UTMD TREATMENT WITH miR-122/ANTI-miR-21 AND DOX CO-TREATMENT DECREASE Hepa1–6 TUMOR GROWTH AND INCRESASE APOPTOSIS *IN VIVO*

The response of Hepa1–6 tumors to UTMD-mediated delivery of miRNA-loaded NPs followed by intraperitoneal injection of Dox was studied by following the scheme shown in Fig. 4A. Treatment significantly decreased the growth of Hepa1–6 tumors compared to untreated controls as observed on day 2 (142.6% relative tumor volume in control *vs.* 110.3% in treated tumors, p=0.008), day 4 (196.5% *vs.* 156.5%, p=0.032), and day 6 (265.2% *vs.* 161.0%, p=0.005) (Fig. 4B). The smaller tumor volume upon treatment was accompanied by a significant increase in cell death (4.3-fold increase, p=0.001) (Fig. 4C,D). Compared to previous studies performed with human HepG2 tumors in immune-compromised nude mice, untreated control Hepa1–6 tumors grew more slowly than HepG2 tumors (29), which could be due to the role of active immune microenvironment in C57BL/6J mice. The reduced growth rate of treated Hepa1–6 tumors was similar to that of treated HepG2 tumors confirming the consistency of therapeutic efficacy by the combination therapy.

Hepa1–6 TUMORS EXPRESS HCC-RELATED CYTOKINES

To characterize the immune condition of Hepa1–6 tumors in the syngeneic C57BL/6J immunocompetent mouse background, we performed a systematic screening for a panel of cytokines with pro- and antitumor functions. All screened cytokines were expressed at seemingly higher levels in the Hepa1–6 tumor tissues engrafted onto the lower flanks of

C57BL/6J mice than in the hind limb muscles of control mice, whereof eight HCC-related cytokines were expressed at significantly increased levels: IL-1α (16.1 *vs.* 3.2 pg/mL, p=0.020), IL-1β (22.4 *vs.* 4.3 pg/mL, p=0.001), IL-5 (44.9 *vs.* 3.4 pg/mL, p=0.001), IL-17 (216.3 *vs.* 3.7 pg/mL, p=0.004), TNF-α (43.2 *vs.* 1.5 pg/mL, p=0.032), macrophage inflammatory protein 1α (MIP-1α) (477.7 *vs.* 16.6 pg/mL, p=0.001), granulocyte-macrophage colony-stimulating factor (GM-CSF) (128.4 *vs.* 2.6 pg/mL, p=0.0001) and Regulated on Activation, Normal T Cell Expressed and Secreted (RANTES) (182.5 *vs.* 13.9 pg/mL, p=0.006) (Fig. 5A). IL-1α is a mediator of liver tumorigenesis (30). IL-1β is overexpressed in human hepatoma cell lines and mediates inflammation, carcinogenesis, invasiveness, and immunosuppression (31,32). IL-5 was associated with poor prognosis in HCC as serum levels of IL-5 were higher in patients with HCC than in healthy controls (33). IL-17 was upregulated in HCC patients suggesting a protumoral function, which has not been understood yet (33). TNF-α is overexpressed in HCC patients, and induces hepatocyte apoptosis and carcinogenesis (34). MIP-1α is overexpressed in HCC mouse models and triggers monocyte migration (32). GM-CSF is frequently upregulated in cancer, and neutralization of GM-CSF inhibits HCC progression and myeloid-derived suppressor cell accumulation (35,36). The pro-inflammatory cytokine RANTES was shown to be overexpressed in patients with chronic liver disease and in HCC mouse models, and its deletion reduces immune cell infiltration and angiogenesis (37). The expression of these protumoral cytokines confirmed the establishment of an HCC-related immune microenvironment upon engraftment of Hepa1–6 tumors.

In tumor-associated lymph nodes, we observed a significant increase in the concentration of several cytokines compared to normal lymph nodes: protumoral IL-1α (38.2 *vs.* 13.8 pg/mL, p=0.008), IL-1β (64.6 *vs.* 34.5 pg/mL, p=0.044), IL-5 (70.1 *vs.* 28.8 pg/mL, p=0.021), IL-6 (35.3 *vs.* 7.0 pg/mL, p=0.029), and antitumoral IL-2 (30.7 *vs.* 13.7 pg/mL, p=0.037), IL-12 (118.4 *vs.* 50.7 pg/mL, p=0.036), and IFN-γ (38.2 *vs.* 8.7 pg/mL, p=0.035) (Fig. 5B). IL-6 that activates STAT3 in the tumor microenvironment inhibiting dendritic cell maturation and blocking antitumor immunity has been reported to be upregulated in HCC patients (38). IL-2 regulates survival, proliferation, and differentiation of T cells and Natural Killer cells for cancer immune surveillance (39). IL-12 is a pro-inflammatory cytokine with antitumor functions such as enhancement of cytotoxic T cells and cytolytic Natural Killer cells, and inhibition of angiogenesis (40). IFN-γ is a pro-inflammatory chemokine enhancing T cell and Natural Killer cell infiltration and tumor cell death in HCC (41). Thus, the inflammatory condition in the tumor tissue seemed to elicit immune system activation in proximal lymph nodes producing both pro- and antitumoral cytokines indicating a fight between immune surveillance and evasion.

In the serum of tumor-bearing mice, IL-3 (3.4 *vs.* 1.8 pg/mL in control, p=0.001) and IL-4 (4.2 *vs.* 1.6 pg/mL in control, p=0.001) were significantly upregulated compared to serum of normal mice (Fig. 5C). IL-3 is a regulator of immune cell growth, differentiation, migration and effector function, and it has been shown to enhance viability and proliferation of leukemic cells (42). IL-4 is involved in M2 macrophage polarization and was associated with cancer cell proliferation and survival in human glioma, ovarian, lung, breast, pancreatic, colon, and bladder cancers (43). Although the exact function of IL-3 and IL-4 in

HCC has not been understood, the data suggests a protumoral cytokine profile in the serum of tumor-bearing mice.

Taken together the data suggests an HCC-specific inflammatory immune microenvironment in Hepa1–6 tumors that is extended to tumor-associated lymph nodes and the systemic circulation.

miRNA and UTMD COMBINATION THERAPY SUPPRESS PROTUMORAL CYTOKINES IN HCC TUMORS

Dox is an FDA-approved chemotherapy whose therapeutic efficacy and immune-modulatory effects have been extensively studied. Here, we focus on evaluating the immune-regulatory effects of UTMD-mediated delivery of miR-122/anti-miR-21-loaded PLGA-NPs in HCC.

We observed that protumoral GM-CSF significantly decreased at 0.5 h after UTMD-mediated miRNA delivery in the treated tumor compared to untreated control tumor (26.5 *vs.* 128.4 pg/mL, p=0.039). Thus, miRNA delivery seemed to elicit antitumoral effects in the tumor tissue.

In the tumor lymph nodes, the concentration of many cytokine levels increased at 0.5 h and at 24 h while concentrations were lower than the control at 6 h post treatment by miRNA delivery. A significant decrease in concentration at 6 h post treatment was observed for: protumoral IL-1α (5.1 *vs.* 38.2 pg/mL, p=0.03), IL-1β (5.7 *vs.* 64.6 pg/mL, p=0.014), IL-5 (6.4 *vs.* 70.1 pg/mL, p=0.009), IL-6 (1.8 *vs.* 35.3 pg/mL, p=0.044) and IL-17 (12.4 *vs.* 86.3 pg/mL, p=0.021), and antitumoral IL-2 (3.5 *vs.* 30.7 pg/mL, p=0.014) and IL-12 (23.0 *vs.* 118.4 pg/mL, p=0.021) (Fig. 6). Interestingly, almost all of these same cytokines were significantly upregulated at 24 h post miRNA delivery: protumoral IL-1α (110.0 *vs.* 38.2 pg/mL, p=0.019), IL-1β (199.9 *vs.* 96.2 pg/mL, p=0.009), IL-5 (137.3 *vs.* 70.1 pg/mL, p=0.039), IL-6 (126.5 *vs.* 35.3 pg/mL, p=0.024), IL-10 (47.8 *vs.* 16.6 pg/mL, p=0.024) and IL-17 (168.5 *vs.* 86.3 pg/mL, p=0.031), and antitumoral IL-2 (79.9 *vs.* 30.7 pg/mL, p=0.007) (Fig. 6). IL-10 mediates M2 macrophage polarization and promotes HCC progression (19). Thus, there was an initial drop followed by upregulation of both pro- and antitumoral cytokines in tumor lymph nodes, which can potentially affect the therapy response (Fig. 6).

In the serum of tumor-bearing mice, miRNA delivery led to an increase of antitumoral IL-2 concentration at 6 h post treatment (13.9 *vs.* 3.3 pg/mL, p=0.008), and an increase in protumoral RANTES concentration at 0.5 h (61.6 *vs.* 32.2 pg/mL, p=0.043), at 6 h (357.9 *vs.* 32.2 pg/mL, p=0.011), and at 24 h (120.3 *vs.* 32.2 pg/mL, p=0.013) (Fig. 6). Thus, there was an overall positive therapy response upon UTMD treatment in the presence of miRNAs.

Taken together, cytokine screening demonstrated an important immune-modulatory potential of UTMD-mediated miRNA therapy, as several HCC-related pro- and antitumoral cytokines were modulated in tumor tissue, adjacent lymph nodes and serum.

UTMD AND miRNA-LOADED NPs SYNERGISTICALLY ACTIVATE IMMUNE RESPONSES

To understand whether UTMD has any contribution to the immune-modulatory effects of miR-122/anti-miR-21 treatment, UTMD treatment alone and UTMD-mediated miRNA

delivery were directly compared. An overview on the concentration changes upon both treatment regimens for all cytokines of the screening panel is presented in Fig. S2. Here, we present the data only for cytokines for which significant concentration changes were observed. In tumor tissue, GM-CSF concentration decreased early upon miRNA delivery (at 0.5 h) and returned to the original level at 24 h post treatment (Fig. 7A). UTMD treatment alone showed a moderate increase in GM-CSF level, but was not significantly different from the control. In tumor lymph nodes, miRNA delivery initially led to a marginal upregulation of cytokines at the earliest time point (0.5 h post treatment) and then to a significant decrease in concentration of IL-1α, IL-1β, IL-2, IL-5, IL-6, IL-12, and IL-17 at 6 h followed by a significant upregulation compared to the control at 24 h. In comparison, UTMD treatment alone triggered moderate but non-significant changes in the concentration of these cytokines that reflected the same tendency of changes as triggered by the UTMD-mediated miRNA delivery.

At 6 h, UTMD treatment alone triggered a significant decrease in IL-5 concentration by 78±9% (mean ± SEM) and miRNA delivery by 91±7%. Moreover, UTMD treatment significantly increased the concentration of IL-12 (341±173%) and of IL-17 (169±33%) at 0.5 h post treatment while miRNA along with UTMD did not add much to the expression of these cytokines (IL-12 to 139±78% and of IL-17 to 131±83%). With regard to TNF-α, UTMD treatment triggered a significant increase (189±33%) at 0.5 h post treatment while UTMD-mediated miRNA delivery showed no effect (72±39%). For GM-CSF, UTMD treatment significantly reduced its concentration by 83±5%, and miRNA supplementation further reduced its concentration (by 58±36%). RANTES was significantly upregulated at 6 h and 24 h upon UTMD treatment (186±34% and 153±17%, respectively), but there was no significant change with UTMD-miRNA delivery (104±22% and 88±20%, respectively). Overall, UTMD showed the same tendency but weaker effects than miRNA delivery suggesting that mechanical US activity contributed to the immune-regulatory effects of miR-122/anti-miR-21 delivery not only by indirectly enhancing the penetration of miRNA-loaded NPs, but also by directly interfering with the immune microenvironment.

In the serum of tumor-bearing mice, significant concentration changes upon miRNA delivery were observed for IL-2 and RANTES while UTMD treatment alone did not trigger any change (Fig. 7C). GM-CSF was significantly reduced (6±2%) at 6 h post UTMD treatment alone, and miRNA supplementation caused only a moderate decrease (55±36%). Thus, there was only a partial overlap in the effect of UTMD alone and UTMD-mediated miRNA delivery. UTMD alone had a much weaker effect, which is coherent with the fact that cytokine-secreting cells in the blood are well exposed to intravenously administered miRNA-loaded NPs, but not to locally applied US.

miRNA DELIVERY TRIGGERS LOCAL AND SYSTEMIC IMMUNE RESPONSES

To assess systemic responses, mice bearing Hepa1–6 tumors on both the right and left hind limbs were used for the study. We treated one tumor with UTMD, but treated and untreated contralateral tumor tissues with their respective adjacent inguinal lymph nodes were collected for cytokine screening. Significant changes in cytokine concentrations upon miRNA delivery were detected in lymph nodes of contralateral tumors while no changes

were observed in the contralateral tumor tissue itself. An overview on concentration changes upon therapy for all cytokines of the screening panel is presented in Fig. S3. Here, significant concentration changes are described (Fig. 8).

GM-CSF concentration reduced in the lymph nodes of the contralateral tumors at 6 h post miRNA delivery while there were no significant changes in the lymph nodes of treated tumors (23.1 (treated) or 13.1 (contralateral) *vs.* 55.0 pg/mL (control), p=0.149 or p=0.043) (Fig. 8). For IL-12 and IL-17, UTMD-mediated miRNA delivery triggered a significant drop in concentration in lymph nodes of both treated tumors and contralateral tumors at 6 h post treatment (IL-12: 23.0 (treated) or 32.7 (contralateral) *vs.* 118.4 pg/mL (control), p=0.021 or p=0.014; IL-17: 12.4 (treated) or 27.1 (contralateral) *vs.* 86.3 pg/mL (control), p=0.021 or p=0.043). For IL-3, a significant upregulation was observed in the lymph nodes of contralateral tumors at 24 h post miRNA delivery while there was no significant change observed in the lymph nodes of treated tumors (46.0 (treated) or 46.8 (contralateral) *vs.* 15.0 pg/mL (control), p=0.051 or p=0.040). Thus, the significant increase in IL-3 and decrease in GM-CSF in contralateral lymph nodes were accompanied by a moderate increase and decrease, respectively, in lymph nodes of treated tumors. In summary, miRNA delivery proved to immunomodulate lymph nodes adjacent to both treated and untreated contralateral tumors therefore suggesting local and systemic therapy effects.

Discussion

In this study, using an immune-competent mouse model bearing subcutaneously engrafted syngeneic Hepa1–6 HCC tumors, we showed: (i) UTMD-mediated delivery restores tumor suppressor miR-122 while depleting the function of oncogenic miR-21 in HCC, (ii) miRNA delivery increases apoptosis *in vitro* and *in vivo*, and reduced tumor growth *in vivo*, and (iii) the tumor immune microenvironment is modulated by partially activating antitumoral cytokines and suppressing protumoral cytokines.

We hypothesized that supplementation of miR-122 and depletion of miR-21 can reactivate antitumor immune functions. The results of our study confirmed this hypothesis by indicating a change in the concentration of pro-inflammatory and protumoral cytokines and suggesting a positive therapy outcome upon treatment. But it is not clear whether the positive effects, such as the upregulation of antitumoral IL-2 can dominate concomitant negative effects, such as the upregulation of HCC-promoting IL-6 and IL-10, and reactivate antitumoral immune responses. Based on cytokine functions, one might assume that M2 macrophages (polarized by IL-10), myeloid-derived suppressor cells (stimulated by GM-CSF), regulatory T cells (activated by IL-1α), and eosinophils (modulated by IL-5) are present in the microenvironment of Hepa1–6 tumors which can be tuned by modulating cytokine expressions to achieve antitumoral effects and impair HCC progression. Our combination therapy triggered local and systemic changes in cytokines levels. This observation was very promising for the development of a therapy approach that directly targets the primary tumor but can also show effect on metastatic nodules in distant sites, which needs further validation. A limitation of our study is the fact that various cytokines in different groups with small sample sizes were analyzed. However, our results show that despite a small sample size significant expression changes could be detected for multiple

cytokines upon therapy. Therefore, we decided to not extend this study to a larger scale. The study was limited to cytokine analysis within the first 24 h upon UTMD-mediated miRNA delivery. Further studies with extended time points with multiple treatment conditions are needed to confirm these assumptions and to understand the long-term changes in the immune microenvironment of HCC after repeated treatment. A characterization of immune cell populations in addition to cytokine profiles will also be useful to allow for an even better understanding of the therapy's immunomodulatory potential for cancer cell elimination.

As expected, UTMD interfered with the tumor's immune microenvironment upon therapy. Indeed, UTMD alone triggered a change in various cytokine concentrations. This is in line with previous studies showing that pulsed focused US triggers mechanical effects and damages tissues at the subcellular level, thereby releasing danger signals, and enables penetration of dendritic cells, activated cytotoxic T cells, and Natural Killer cells into tumor tissues resulting in a decrease of tumor growth (44–46).

PLGA-NPs are clinically approved as they show good biocompatibility and provide high delivery efficacy, and miRNA-loaded PLGA-NPs can be prepared according to Good Manufacturing Practice (GMP), which facilitates rapid clinical translation of this approach. UTMD has already been shown to be safe and efficient for the delivery of chemotherapy in patients with inoperable pancreatic cancer in a first human clinical trial (47). With regard to these facts, our therapy approach has a good chance to be clinically translatable in the future, but requires first experimental clinical trials to prove these assumptions.

To further fine-tune and enhance our therapy approach, it could be complemented with additional drugs such as antitumoral IL-2 protein, which was previously observed to be downregulated in our therapy approach, and for which different clinically translatable drug formats are available. Also, the combination of UTMD-mediated delivery of targeted gene therapy with immunotherapies is conceivable. Recent studies from Ferrara and colleagues have shown a local and systemic tumor responses after treatment with US-mediated hyperthermia for delivery of Dox-encapsulated temperature-sensitive liposomes combined with intra-tumoral injection of toll-like receptor-9 activating CpG immunotherapy or intraperitoneal injection of anti-PD-1 immune checkpoint inhibitor antibodies (48,49). Further studies are needed to investigate whether combined UTMD drug delivery and immunotherapy can have mutually intensified therapeutic effects that can be exploited for cancer therapy.

The therapy approach shown in this study targets a common oncogenic miRNA and complements a common tumor suppressor miRNA. Besides HCC, dysregulation of miR-122 and miR-21 were also found in other solid tumors such as, breast cancer, pancreatic cancer and prostate cancer (50), which could potentially benefit from the development of our drug delivery approach as tumors in these respective organs can be easily insonified, opening a path for broad clinical utility that warrants further assessment.

In conclusion, UTMD-mediated delivery of miR-122/anti-miR-21-loaded PLGA-NPs for the treatment of HCC is a powerful strategy. In addition to a sensitization of tumor cells to apoptosis and a reduction in tumor growth, activation of antitumoral immune functions was

also observed. Further studies will be required to determine whether the effects are long-lasting and translate into changes in immune cell populations, how to fine-tune and enhance therapeutic efficacy by combining with anticancer drugs, and whether this strategy can be adopted to other types of cancer. The combination therapy exploiting biophysical effects and molecular targeting of relevant oncogenes/tumor suppressors provides an optimistic approach for countering aggressiveness and resistance of HCC to improve therapeutic outcome in patients.

Supplementary Material

Refer to Web version on PubMed Central for supplementary material.

Acknowledgements

The authors thank Prof. Dr. Juergen K. Willmann who initiated and managed this study in 2016/2017. He passed away in 2018, but this work could not have been conducted without his thoughtful initiative.

Financial Support

This research was in part supported by NIH R01CA209888. We thank Canary Center at Stanford, Department of Radiology for facility and resources. We also thank SCi^3 small animal imaging service center, Stanford University School of Medicine for providing imaging facilities and data analysis support. The first author was supported by the LabEx DEVweCAN (ANR-10-LABX-0061) of the University of Lyon, within the program "Investissements d'Avenir" (ANR-11-IDEX-0007) operated by the French National Research Agency (ANR), by the German-American Fulbright Commission, by the France-Stanford Center for Interdisciplinary Studies, and by NIH R01CA155289.

List of Abbreviations

anti-miR-21	anti-microRNA-21
Dox	doxorubicin
GM-CSF	granulocyte-macrophage colony-stimulating factor
HCC	hepatocellular carcinoma
IL	interleukin
MB	microbubble
MIP-1α	macrophage inflammatory protein 1α
miR-122	microRNA-122
miRNA	microRNA
NP	nanoparticle
PLGA	poly (lactic-*co*-glycolic acid)
RANTES	Regulated on Activation, Normal T Cell Expressed and Secreted
US	ultrasound

UTMD	ultrasound-targeted microbubble destruction

References

1. Forner A, Llovet JM, Bruix J. Hepatocellular carcinoma. Lancet. 2012;379:1245–1255. [PubMed: 22353262]
2. European Association for Study of Liver, European Organisation for Research and Treatment of Cancer. EASL-EORTC clinical practice guidelines: management of hepatocellular carcinoma. Eur. J. Cancer 2012;48:599–641. [PubMed: 22424278]
3. Lencioni R, Cioni D, Crocetti L, Bartolozzi C. Percutaneous ablation of hepatocellular carcinoma: state-of-the-art. Liver Transpl. 2004;10:S91–97. [PubMed: 14762847]
4. Yang T, Zhang J, Lu J-H, Yang L-Q, Yang G-S, Wu M-C, et al. A new staging system for resectable hepatocellular carcinoma: comparison with six existing staging systems in a large Chinese cohort. J. Cancer Res. Clin. Oncol 2011;137:739–750. [PubMed: 20607551]
5. Llovet JM, Fuster J, Bruix J. Intention-to-treat analysis of surgical treatment for early hepatocellular carcinoma: resection versus transplantation. Hepatology. 1999;30:1434–1440. [PubMed: 10573522]
6. Llovet JM, Bruix J. Systematic review of randomized trials for unresectable hepatocellular carcinoma: Chemoembolization improves survival. Hepatology. 2003;37:429–442. [PubMed: 12540794]
7. Raoul J-L, Sangro B, Forner A, Mazzaferro V, Piscaglia F, Bolondi L, et al. Evolving strategies for the management of intermediate-stage hepatocellular carcinoma: available evidence and expert opinion on the use of transarterial chemoembolization. Cancer Treat. Rev. 2011;37:212–220. [PubMed: 20724077]
8. Giglia JL, Antonia SJ, Berk LB, Bruno S, Dessureault S, Finkelstein SE. Systemic therapy for advanced hepatocellular carcinoma: past, present, and future. Cancer Control. 2010;17:120–129. [PubMed: 20404795]
9. Llovet JM, Ricci S, Mazzaferro V, Hilgard P, Gane E, Blanc J-F, et al. Sorafenib in advanced hepatocellular carcinoma. N. Engl. J. Med 2008;359:378–390. [PubMed: 18650514]
10. Keenan BP, Fong L, Kelley RK. Immunotherapy in hepatocellular carcinoma: the complex interface between inflammation, fibrosis, and the immune response. J Immunother Cancer. 2019;7:267. [PubMed: 31627733]
11. Wang T-Y, Choe JW, Pu K, Devulapally R, Bachawal S, Machtaler S, et al. Ultrasound-guided delivery of microRNA loaded nanoparticles into cancer. J Control Release. 2015;203:99–108. [PubMed: 25687306]
12. Mullick Chowdhury S, Wang T-Y, Bachawal S, Devulapally R, Choe JW, Abou Elkacem L, et al. Ultrasound-guided therapeutic modulation of hepatocellular carcinoma using complementary microRNAs. J Control Release. 2016;238:272–280. [PubMed: 27503707]
13. Wang T-Y, Wilson KE, Machtaler S, Willmann JK. Ultrasound and Microbubble Guided Drug Delivery: Mechanistic Understanding and Clinical Implications. Curr Pharm Biotechnol. 2014;14:743–752.
14. Fornari F, Gramantieri L, Giovannini C, Veronese A, Ferracin M, Sabbioni S, et al. MiR-122/cyclin G1 interaction modulates p53 activity and affects doxorubicin sensitivity of human hepatocarcinoma cells. Cancer Res. 2009;69:5761–5767. [PubMed: 19584283]
15. Coulouarn C, Factor VM, Andersen JB, Durkin ME, Thorgeirsson SS. Loss of miR-122 expression in liver cancer correlates with suppression of the hepatic phenotype and gain of metastatic properties. Oncogene. 2009;28:3526–3536. [PubMed: 19617899]
16. Xu G, Zhang Y, Wei J, Jia W, Ge Z, Zhang Z, et al. MicroRNA-21 promotes hepatocellular carcinoma HepG2 cell proliferation through repression of mitogen-activated protein kinase-kinase 3. BMC Cancer. 2013;13:469. [PubMed: 24112539]
17. Meng F, Henson R, Wehbe–Janek H, Ghoshal K, Jacob ST, Patel T. MicroRNA-21 Regulates Expression of the PTEN Tumor Suppressor Gene in Human Hepatocellular Cancer. Gastroenterology. 2007;133:647–658. [PubMed: 17681183]
18. Prieto J, Melero I, Sangro B. Immunological landscape and immunotherapy of hepatocellular carcinoma. Nat Rev Gastroenterol Hepatol. 2015;12:681–700. [PubMed: 26484443]

19. Ambade A, Satishchandran A, Saha B, Gyongyosi B, Lowe P, Kodys K, et al. Hepatocellular carcinoma is accelerated by NASH involving M2 macrophage polarization mediated by hif-1αinduced IL-10. Oncoimmunology. 2016;5:e1221557. [PubMed: 27853646]
20. Li C, Deng M, Hu J, Li X, Chen L, Ju Y, et al. Chronic inflammation contributes to the development of hepatocellular carcinoma by decreasing miR-122 levels. Oncotarget. 2016;7:17021–17034. [PubMed: 26933995]
21. Hsu S-H, Wang B, Kota J, Yu J, Costinean S, Kutay H, et al. Essential metabolic, anti-inflammatory, and anti-tumorigenic functions of miR-122 in liver. J. Clin. Invest 2012;122:2871–2883. [PubMed: 22820288]
22. Sheedy FJ. Turning 21: Induction of miR-21 as a Key Switch in the Inflammatory Response. Front Immunol. 2015;6:19. [PubMed: 25688245]
23. Lu Z, Liu M, Stribinskis V, Klinge CM, Ramos KS, Colburn NH, et al. MicroRNA-21 promotes cell transformation by targeting the programmed cell death 4 gene. Oncogene. 2008;27:4373–4379. [PubMed: 18372920]
24. Liu H-L, Hsieh H-Y, Lu L-A, Kang C-W, Wu M-F, Lin C-Y. Low-pressure pulsed focused ultrasound with microbubbles promotes an anticancer immunological response. J Transl Med. 2012;10:221. [PubMed: 23140567]
25. Sta Maria NS, Barnes SR, Weist MR, Colcher D, Raubitschek AA, Jacobs RE. Low Dose Focused Ultrasound Induces Enhanced Tumor Accumulation of Natural Killer Cells. PLoS ONE. 2015;10:e0142767. [PubMed: 26556731]
26. Bandyopadhyay S, Quinn TJ, Scandiuzzi L, Basu I, Partanen A, Tomé WA, et al. Low-Intensity Focused Ultrasound Induces Reversal of Tumor-Induced T Cell Tolerance and Prevents Immune Escape. J. Immunol 2016;196:1964–1976. [PubMed: 26755821]
27. Devulapally R, Foygel K, Sekar TV, Willmann JK, Paulmurugan R. Gemcitabine and Antisense-microRNA Co-encapsulated PLGA-PEG Polymer Nanoparticles for Hepatocellular Carcinoma Therapy. ACS Appl Mater Interfaces. 2016;8:33412–33422. [PubMed: 27960411]
28. Devulapally R, Sekar NM, Sekar TV, Foygel K, Massoud TF, Willmann JK, et al. Polymer nanoparticles mediated codelivery of antimiR-10b and antimiR-21 for achieving triple negative breast cancer therapy. ACS Nano. 2015;9:2290–2302. [PubMed: 25652012]
29. Chowdhury SM, Lee T, Bachawal SV, Devulapally R, Abou-Elkacem L, Yeung TA, et al. Longitudinal assessment of ultrasound-guided complementary microRNA therapy of hepatocellular carcinoma. J Control Release. 2018;281:19–28. [PubMed: 29758233]
30. Sakurai T, He G, Matsuzawa A, Yu G-Y, Maeda S, Hardiman G, et al. Hepatocyte necrosis induced by oxidative stress and IL-1 alpha release mediate carcinogen-induced compensatory proliferation and liver tumorigenesis. Cancer Cell. 2008;14:156–165. [PubMed: 18691550]
31. Voronov E, Dotan S, Krelin Y, Song X, Elkabets M, Carmi Y, et al. Unique Versus Redundant Functions of IL-1α and IL-1β in the Tumor Microenvironment. Front Immunol. 2013;4:177. [PubMed: 23847618]
32. Lu P, Nakamoto Y, Nemoto-Sasaki Y, Fujii C, Wang H, Hashii M, et al. Potential interaction between CCR1 and its ligand, CCL3, induced by endogenously produced interleukin-1 in human hepatomas. Am. J. Pathol 2003;162:1249–1258. [PubMed: 12651617]
33. Kim MJ, Jang JW, Oh BS, Kwon JH, Chung KW, Jung HS, et al. Change in inflammatory cytokine profiles after transarterial chemotherapy in patients with hepatocellular carcinoma. Cytokine. 2013;64:516–522. [PubMed: 24035756]
34. Jang M-K, Kim HS, Chung Y-H. Clinical aspects of tumor necrosis factor-α signaling in hepatocellular carcinoma. Curr. Pharm. Des 2014;20:2799–2808. [PubMed: 23944370]
35. Hong I-S. Stimulatory versus suppressive effects of GM-CSF on tumor progression in multiple cancer types. Exp. Mol. Med. 2016;48:e242. [PubMed: 27364892]
36. Lin Y, Yang X, Liu W, Li B, Yin W, Shi Y, et al. Chemerin has a protective role in hepatocellular carcinoma by inhibiting the expression of IL-6 and GM-CSF and MDSC accumulation. Oncogene. 2017;36:3599–3608. [PubMed: 28166197]
37. Mohs A, Kuttkat N, Reiβing J, Zimmermann HW, Sonntag R, Proudfoot A, et al. Functional role of CCL5/RANTES for HCC progression during chronic liver disease. J. Hepatol. 2017;66:743–753. [PubMed: 28011329]

38. Kitamura H, Ohno Y, Toyoshima Y, Ohtake J, Homma S, Kawamura H, et al. Interleukin-6/STAT3 signaling as a promising target to improve the efficacy of cancer immunotherapy. Cancer Sci. 2017;108:1947–1952. [PubMed: 28749573]
39. Sim GC, Radvanyi L. The IL-2 cytokine family in cancer immunotherapy. Cytokine Growth Factor Rev. 2014;25:377–390. [PubMed: 25200249]
40. Whitworth JM, Alvarez RD. Evaluating the role of IL-12 based therapies in ovarian cancer: a review of the literature. Expert Opin Biol Ther. 2011;11:751–762. [PubMed: 21391898]
41. Elia G, Fallahi P. Hepatocellular carcinoma and CXCR3 chemokines: a narrative review. Clin Ter. 2017;168:e37–e41. [PubMed: 28240761]
42. Broughton SE, Dhagat U, Hercus TR, Nero TL, Grimbaldeston MA, Bonder CS, et al. The GM-CSF/IL-3/IL-5 cytokine receptor family: from ligand recognition to initiation of signaling. Immunol. Rev. 2012;250:277–302. [PubMed: 23046136]
43. Setrerrahmane S, Xu H. Tumor-related interleukins: old validated targets for new anticancer drug development. Mol. Cancer. 2017;16:153. [PubMed: 28927416]
44. van den Bijgaart RJE, Eikelenboom DC, Hoogenboom M, Fütterer JJ, den Brok MH, Adema GJ. Thermal and mechanical high-intensity focused ultrasound: perspectives on tumor ablation, immune effects and combination strategies. Cancer Immunol. Immunother. 2017;66:247–258. [PubMed: 27585790]
45. Hu Z, Yang X, Liu Y, Sankin GN, Pua EC, Morse MA, et al. Investigation of HIFU-induced anti-tumor immunity in a murine tumor model. Journal of Translational Medicine. 2007;5:34. [PubMed: 17625013]
46. Lu P, Zhu X-Q, Xu Z-L, Zhou Q, Zhang J, Wu F. Increased infiltration of activated tumor-infiltrating lymphocytes after high intensity focused ultrasound ablation of human breast cancer. Surgery. 2009;145:286–293. [PubMed: 19231581]
47. Dimcevski G, Kotopoulis S, Bjånes T, Hoem D, Schjøtt J, Gjertsen BT, et al. A human clinical trial using ultrasound and microbubbles to enhance gemcitabine treatment of inoperable pancreatic cancer. J Control Release. 2016;243:172–181. [PubMed: 27744037]
48. Kheirolomoom A, Ingham ES, Mahakian LM, Tam SM, Silvestrini MT, Tumbale SK, et al. CpG expedites regression of local and systemic tumors when combined with activatable nanodelivery. J Control Release. 2015;220:253–264. [PubMed: 26471394]
49. Kheirolomoom A, Silvestrini MT, Ingham ES, Mahakian LM, Tam SM, Tumbale SK, et al. Combining activatable nanodelivery with immunotherapy in a murine breast cancer model. J Control Release. 2019;303:42–54. [PubMed: 30978432]
50. Pan X, Wang Z-X, Wang R. MicroRNA-21: a novel therapeutic target in human cancer. Cancer Biol. Ther 2010;10:1224–1232. [PubMed: 21139417]

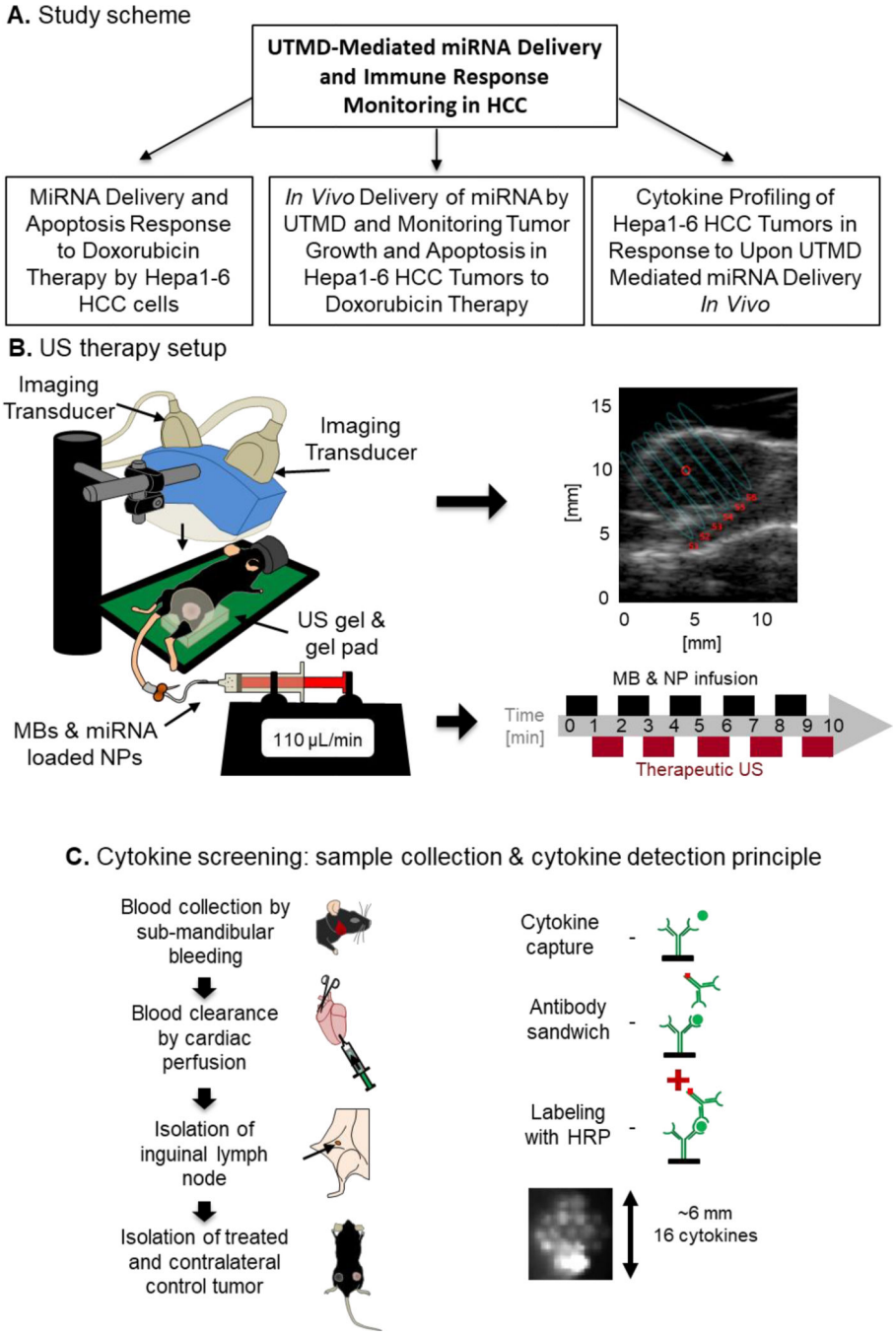

FIG. 1.

Study design. (A) Schematic workflow of the study: In order to study the effect of UTMD-mediated miRNA delivery on the immune response of HCC *in vivo*, the study was performed in three phases. (B) US therapy setup: The US device comprises an imaging transducer for guidance and a therapy transducer for focused mechanical US inducing MB cavitation. The US device is lowered until transducers and tissues are coupled using US gel. B-mode is used to focus the US energy on the center of the tumor. The therapy protocol lasts 10 min with alternating cycles of MB & NP infusion and cavitation. (C) Cytokine screening:

Tumors were treated by UTMD-mediated delivery of miR-122/anti-miR-21-loaded PLGA-NPs. Serum was collected by submandibular bleeding. The blood pool was cleared by cardiac perfusion with PBS and inguinal lymph nodes and tumors were collected. Using a multiplex cytokine array assay, cytokines were captured with anti-cytokine antibodies, immobilized at the bottom of a 96-well plate and revealed like in a Western blot analysis.

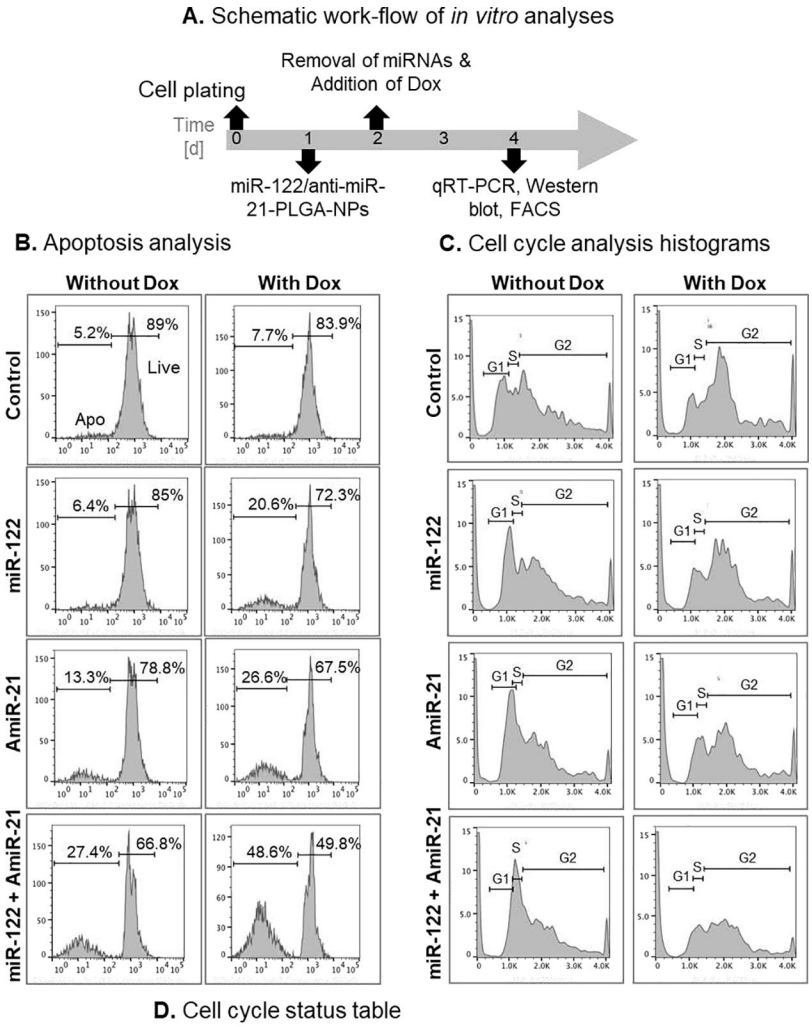

D. Cell cycle status table

	Cell cycle phases [%]		
Condition	**G1**	**S**	**G2**
Control	22.57	19.41	58
Dox	11.55	13.86	74.5
miR-122	18.46	21.89	59.6
miR-122 + Dox	8.4	15.98	75.5
anti-miR-21	18.86	28.2	52.9
anti-miR-21 + Dox	9.2	18.75	72
miR-122 + anti-miR-21	11.47	34.5	53.97
miR-122 + anti-miR-21 + Dox	7.6	19.23	73

FIG. 2.

MiR-122 and anti-miR-21 co-delivery sensitize murine Hepa1–6 cells to Dox and induce apoptosis and cell cycle arrest. (A) Scheme for the timing of various conditions for *in vitro* experiments. (B) FACS histograms after propidium iodide (PI) staining to distinguish between viable and apoptotic cells. (C) FACS histograms showing cell cycle phases in response to treatment. (D) Table showing the percentage of cells in different cell cycle phases in response to different treatment conditions (cells were treated with Dox at 1 μM).

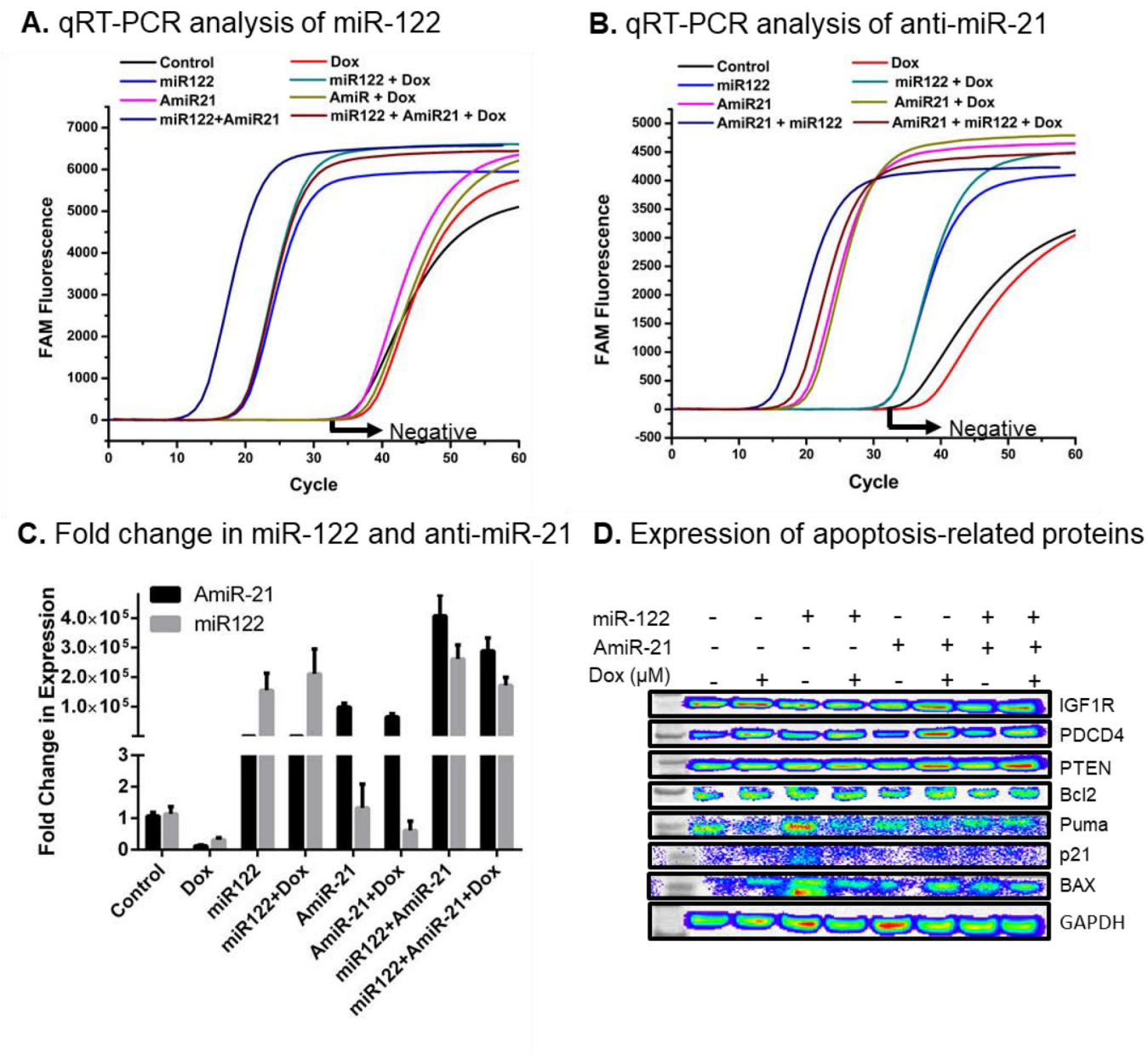

FIG. 3.

Assessment of intracellular miR-122 and anti-miR-21 levels after UTMD, and the expression of apoptosis-related proteins in Hepa1–6 tumor cells after treatment with miR-122/anti-miR-21/Dox. Fluorescence charts indicating the threshold cycles of (A) anti-miR-21 and (B) miR-122 as assessed by quantitative RT-PCR. (C) Quantification of the fold change in delivered intracellular miRNAs levels (anti-miR-21 and miR-122) relative to the control sample. (D) Western blot analysis results of cells treated with a combination of microRNAs in the presence Dox for the expression of pro- and anti-apoptotic proteins along with miRNA targets.

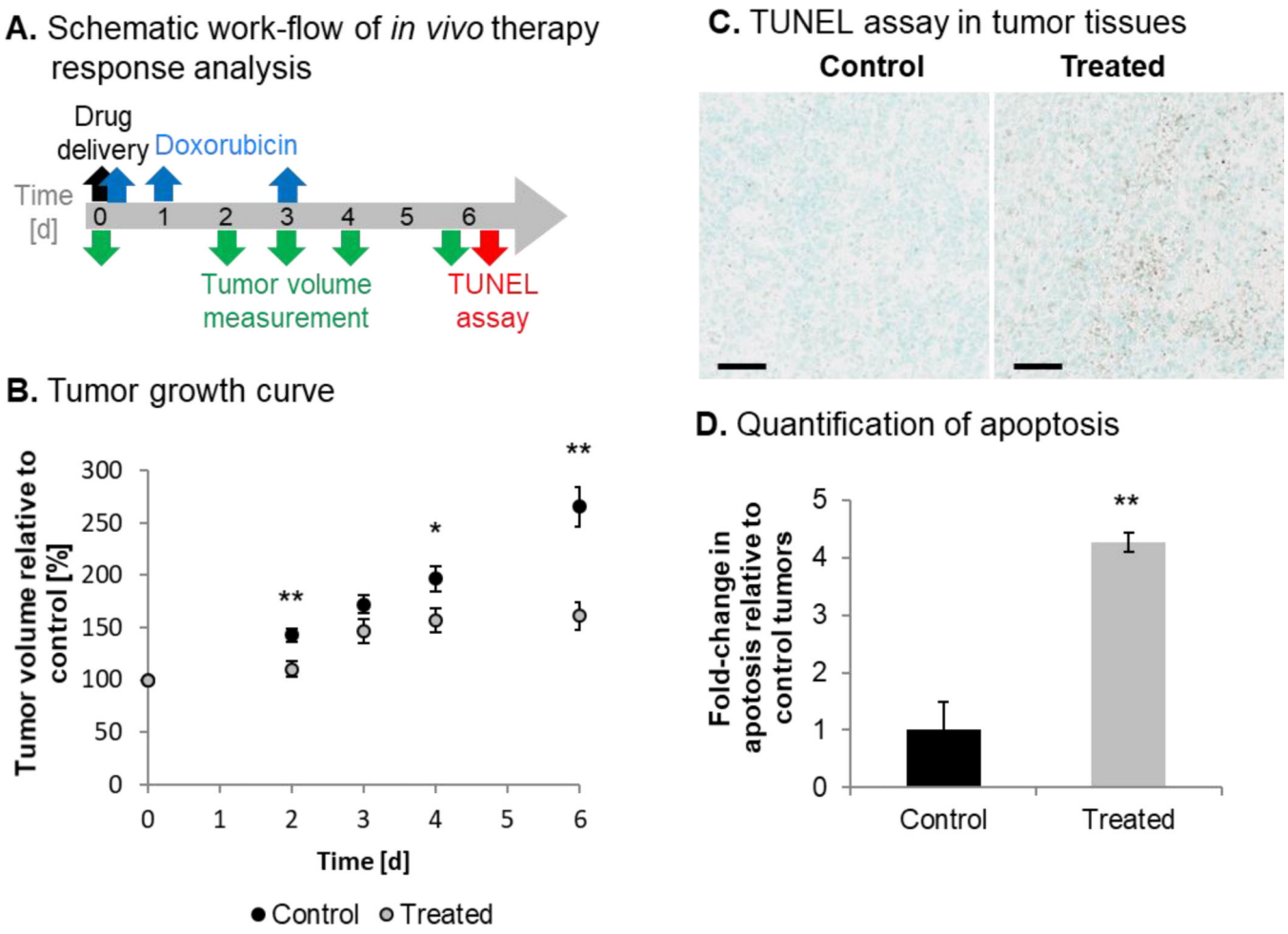

FIG. 4.

Tumor growth and apoptosis in the murine immune-competent Hepa1–6 syngeneic HCC mouse model upon UTMD-mediated miRNA delivery and Dox co-treatment. (A) Schematic illustration of treatment timing of *in vivo* therapy conditions and assessment. (B) Growth curves of untreated control tumors (N=6) and treated tumors (N=10). (C) Representative TUNEL assay results of tumors from control and treated animals. Scale bars indicate 50 μm. (D) Quantified apoptosis staining in control and treated tumor slices (N=3).

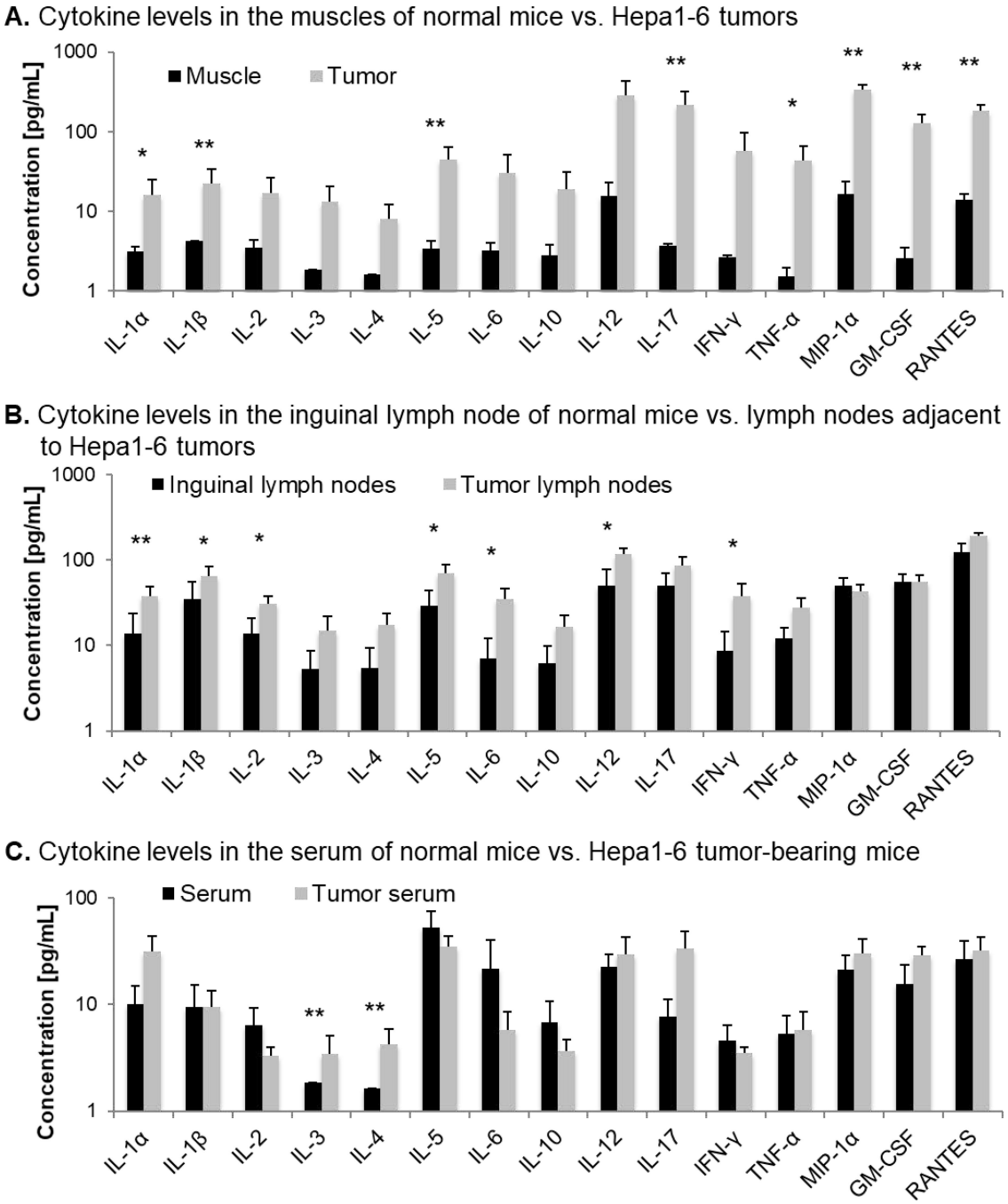

FIG. 5.

Physiological baseline cytokine levels in normal C57BL/6J mice and C57BL/6J mice bearing Hepa1–6 tumors. Comparison of cytokine expression levels (A) in normal hind limb muscle of healthy 12-week-old C57BL/6 mice and syngeneic Hepa1–6 tumors from C57BL/6 mice, (B) in inguinal lymph nodes of normal mice and tumor-associated lymph nodes, and (C) in serum of normal mice and serum of tumor-bearing mice.

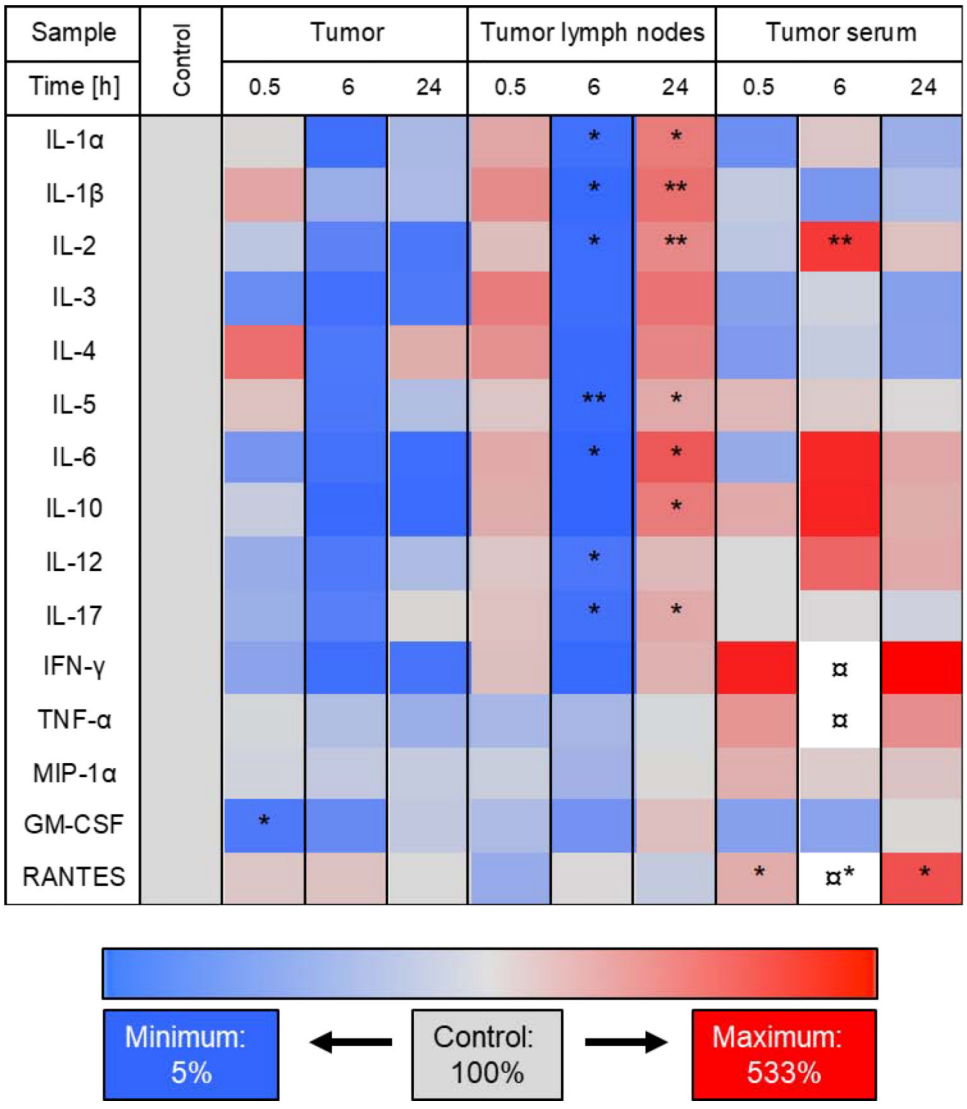

FIG. 6.

Heat map of the screening results of therapy-induced cytokine expression changes in tumors, lymph nodes and serum. Cytokine expressions were assessed in tumors, tumor-associated lymph nodes (tumor lymph nodes) and in serum of tumor-bearing mice (tumor serum) prior to treatment (control) and 0.5, 6, and 24 h after treatment with UTMD-mediated delivery of miR-122-/anti-miR-21-loaded NPs. Decrease in cytokine expression is indicated in blue and increase is shown in red. As a reference, the cytokine expression in control tissues (without treatment) was set to 100% (shown in grey). The currency sign (¤) indicates that the cytokine expression was higher than the depicted maximum of 533% (IFN-γ at 1918%, TNF-α at 921%, RANTES at 1112%). For statistical analysis, all treated samples were compared to the untreated control.

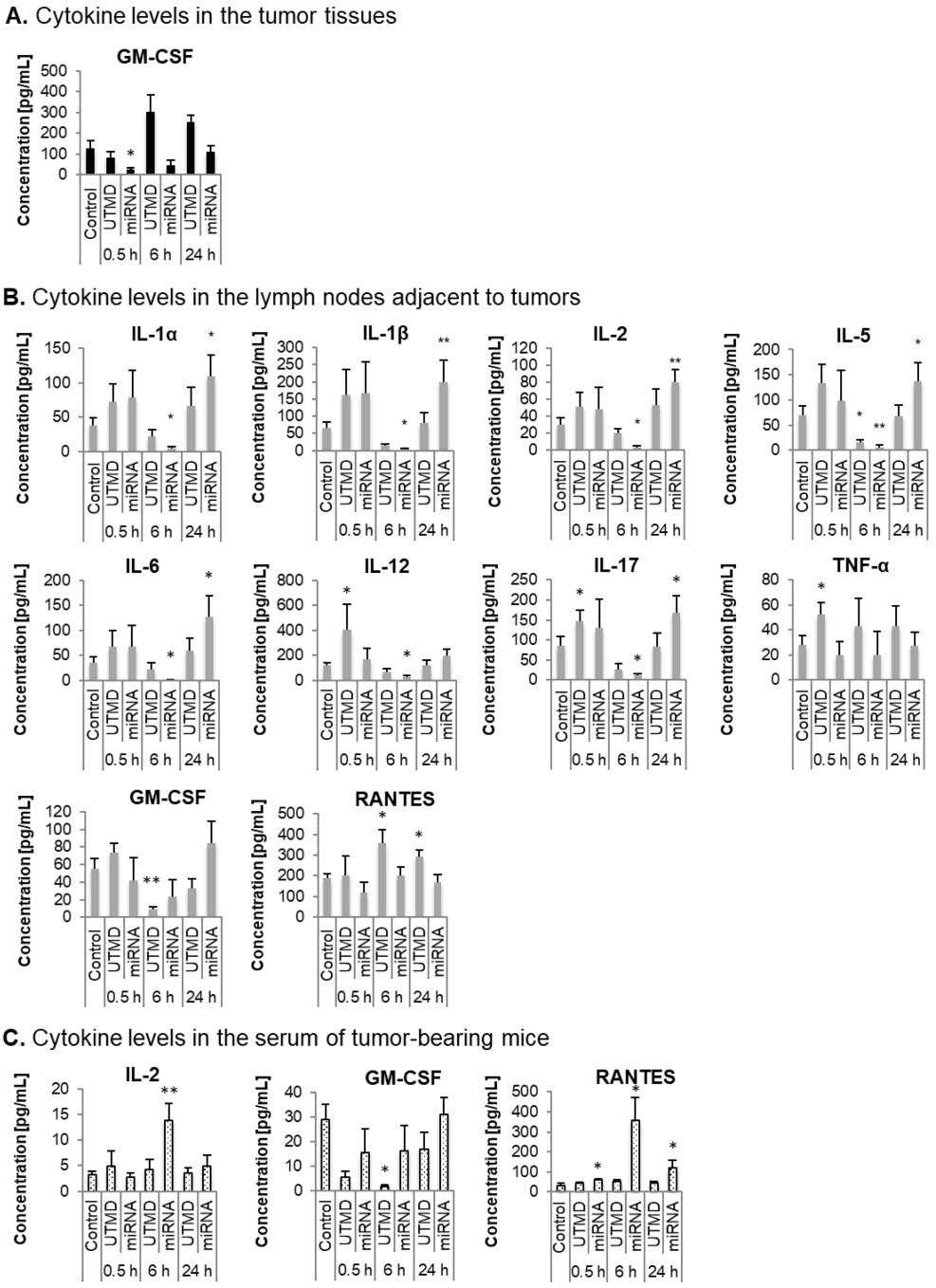

FIG. 7.

Comparison of the cytokine expression changes after UTMD treatment alone or UTD-mediated miRNA drug delivery. Cytokine expressions were assessed in (A) tumors, (B) tumor-associated lymph nodes (tumor lymph nodes) and (C) serum of tumor-bearing mice (tumor serum) prior to treatment (0 h) and 0.5, 6, and 24 h after treatment with UTMD-mediated delivery of miR-122-/anti-miR-21-loaded NPs. For statistical analysis, all treated samples were compared to the untreated control.

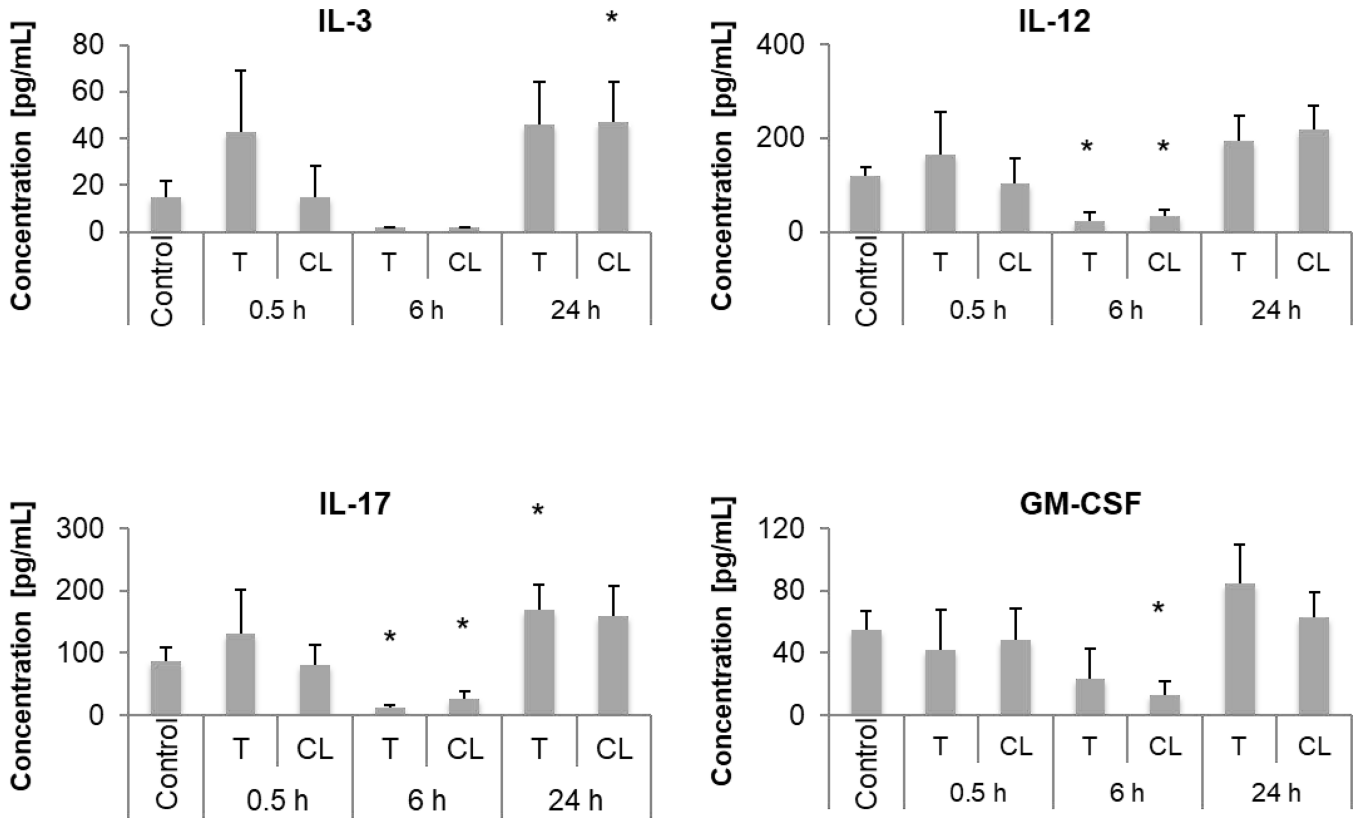

FIG. 8.

Evaluation of systemic cytokine expression changes upon UTMD-mediated miRNA delivery. Mice were engrafted with Hepa1–6 tumors on both hind limbs. Only one tumor was treated (T) while the other was used as a contralateral control (CL). Cytokine expressions were assessed in tumor-associated lymph nodes prior to treatment (control) and 0.5, 6, and 24 h after treatment with UTMD-mediated delivery of miR-122-/anti-miR-21-loaded NPs. For statistical analysis, all treated and contralateral samples were compared to the untreated control.